

Electrochemical switching of conducting polymers: A variable resistance transmission line model

M.R. Warren ^{a,*} J.D. Madden ^b

^a*Department of Physics, Advanced Materials and Engineering Laboratory,
University of British Columbia, Vancouver, British Columbia, Canada*

^b*Department of Electrical and Computer Engineering, Advanced Materials and
Engineering Laboratory, University of British Columbia, Vancouver, British
Columbia, Canada*

Abstract

We present a model to explain some anomalous properties that have been observed in the electrochemical switching of conducting polymers, including: moving phase fronts on charging from the reduced, insulating state; residual charge in the polymer after complete reduction; and, the sharp anodic peak and flattened cathodic peak observed in cyclic voltammograms. The electrochemistry is modeled as a transmission line where the doping-induced metal-insulator transition that occurs in the polymer's electronic conductivity is explicitly included. The transient charges and currents during potentiostatic steps and linear sweeps are solved using the method of finite differences in the time domain. We demonstrate that purely electronic, transmission line models can describe the range of electrochemical behavior of conducting polymers, provided that variation in the parameters with oxidation state is included.

Key words: Conducting polymers, Impedance model, Moving front, Cyclic voltammograms, Polypyrrole

PACS:

1 Introduction

The reversible electrochemical switching of conducting polymers has many applications, including supercapacitors [1,2], electrochromic windows and dis-

* mya@physics.ubc.ca

plays [3], and light-weight, muscle-like actuators [4–7]. For this reason, the electrochemistry of conducting polymers has been studied extensively using techniques including electrochemical impedance spectroscopy (EIS), chronoamperometry and spectroscopic methods. The electrochemistry of conducting polymers has typically been described as a distributed capacitor [8–11]. During redox, charges are created on the polymer backbone and ions flow in and out to balance the charge in a process called electrochemical doping. The entire polymer matrix is a double-layer capacitor. This interpretation has been justified via measurements of the electrochemical impedance, which has been effectively modeled using RC transmission line circuits [12–14].

Interpretation of transient experiments is more complex as changes in oxidation state can cause drastic changes in the electrochemical properties of conducting polymers. The electronic conductivity of the polymer can change by 4-8 orders of magnitude with oxidation state [15,16], from fully metallic in the oxidized state to insulating in the reduced state [17]. Also, the concentration of ions in the polymer causes structural changes [18,19] that likely affect the porosity of the film, and the diffusivity of the ions [20,21].

In a series of papers, Tezuka et. al. present a thorough investigation of the transient behavior of the conducting polymer, polypyrrole. In these experiments, a thin film of polypyrrole was placed on an insulating substrate and electrically connected at one end. During potentiostatic switching, chronoamperograms were recorded and the local charge along the length of the film was monitored through the electrochromic effect with a photodiode array. The authors find that the absorption is proportional to the oxidation state of the film [22]. The experimental geometry is shown in Figure 1. To summarize the results of these experiments:

- When a film is reduced from the oxidized (as-grown) state in the experimental geometry shown in Figure 1, the charge is observed to decrease in a fairly diffusive manner over the length of the film and the current decays monotonically with time. [23]
- It is impossible to fully reduce the film in this geometry. The reduction is stopped when the current is negligible, but 13% of the charge on the film remains. [23]
- In [24], a film is exhaustively reduced on a conductive substrate to eliminate all charges on the polymer, and then reoxidized in the geometry shown in Figure 1. At sufficiently oxidizing potentials, the electrochemical switching exhibits a constant velocity phase front between reduced and oxidized regions moving away from the working electrode. The current is nearly constant until the front reaches the end of the film, when it decays rapidly.
- The time to reoxidize from the fully reduced state in [24] is considerably longer than the time constant for reduction in [23].
- Cyclic voltammograms (CVs) show a sharp anodic peak followed by a large

capacitive current, and a very broad cathodic peak. [22]

The front phenomenon has been of particular interest, and there have been many theoretical studies to explain it. Tezuka presents an electrochemical model where the electron kinetics at the boundary between oxidized and reduced regions is the limiting step [25]. Lacroix [26] and others [27–29] assume that ionic transport is the rate limiting step. They present a mass-transport model where the front is caused by ion migration at the conductive/non-conductive interface. Each of these models produces a moving phase front, but because of their limiting case assumptions, none have been able to explain the full range of conducting polymer electrochemistry that has been observed in Tezuka’s experiments. Typically, separate theories have been required to describe the fronts, the reduction behavior and the characteristic shape of CVs [25,23,22].

This paper presents a model which is able to explain the range of electrochemical behavior observed in Tezuka’s experiments described above. In the variable resistance transmission line model (VRTL), conducting polymer charging is modeled as an RC transmission line similar to standard EIS models, but it explicitly includes the changes in electronic mobility that occur during electrochemical switching.

2 Description of the Model

The electrochemistry of conducting polymers can be described by a transmission line composed of resistor elements for the ionic (r_i) and electronic (r_P) mobilities, and capacitive elements (c) for the charge capacity of the film. The particular combination of these elements in a transmission line model is a function of the experimental geometry of the working electrode, but in theory any experiment may be modeled in this fashion.

For example, the transmission line model corresponding to Tezuka’s experiments is shown schematically in Figure 2. The length of the transmission line represents the length of the film perpendicular to the working electrode. The length is discretized into N branches labeled i from 1 to N from the working electrode. In this geometry, the ion transport occurs predominantly in parallel over the area of the film, and the electron transport is predominantly in series along the length of the film. The charging through the film thickness is modeled as a lumped parameter RC branch. This is a simplification, as charging through the thickness is a distributed process that should be represented by a transmission line in its own right; this is shown schematically in the upper box in Figure 2. The simplification is valid in this study, however, as we are interested in time-scales greater than the time constant for charging through the

thickness of the film, τ . At $t > \tau$, the transmission line through the thickness behaves like an RC circuit. Note that this approximation is *not* valid when the resistance over the length of the film is much smaller than the ionic resistance through the thickness, such as when the film is in contact with a conductive substrate. In cases such as these, the full transmission line representation for charging through the thickness is easily incorporated. In addition, we neglect the surface capacitance of the film, which will also affect the short time-scale response of the model.

The electronic conductivity of the polymer is known to be a sigmoidal function of the oxidation state [15]. This is described in Equation 1:

$$\sigma = \frac{\sigma_{max} - \sigma_{min}}{1 + e^{-(q-q_0)/w}} + \sigma_{min} \quad (1)$$

where σ_{max} , σ_{min} , q , q_0 and w are the conductivity in the oxidized and the reduced state, the oxidation state or charge on the polymer, the charge at which the polymer switches between conductive and non-conductive states, and the width of the transition respectively. $q = 0$ in the reduced state, and $q = q_{max}$ in the oxidized state, where q_{max} depends on the capacitance of the film and the oxidizing potential. Note that Equation 1 is simply a representative sigmoidal function, and the actual conductivity profile of a particular polymer is highly dependent on the deposition conditions and should be measured for each polymer system. This relationship is incorporated in the model via a variable polymer resistance $r_P(q)$. The resistance at each position i is a function of the local oxidation state, or the charge on capacitor c_i .

Because of the variability of the electronic conductivity, an analytic solution cannot be found for this model, and the transient behavior during a potential step experiment is solved using the method of finite differences. The algorithm is as follows:

- (1) Input parameters are the initial and final voltage in the step potential, V_0 and V_f . In this model, $V_{red} = 0V$ is the fully reduced state (-0.8V vs. SCE), and $V_{ox} = 1.2V$ is the fully oxidized state (0.4V vs. SCE).
- (2) A transmission line circuit is constructed with a finite number of elements, N . N is chosen such that the solution converges (usually around 100).
- (3) V_0 is used to determine the initial steady state charge on each of the capacitors, $q_i(t = 0) = cV_0$. The charges are used to determine the initial electronic resistance of the polymer at position i using Equation 1.
- (4) The instantaneous currents, i_i , in each branch are calculated based on the impedance from the previous step and the step potential, V_f .
- (5) The time step, dt , is implemented: the charge on the capacitors is changed by an amount $q_i(t + dt) = q_i(t) + i_i(t)dt$ and the resistances are updated based on the new charges $q_i(t)$. The magnitude of dt is also chosen such

that the simulation converges.

- (6) 4 and 5 are repeated until the current decays to zero and the system has attained equilibrium.

The simulations take only a couple of minutes to perform and give both the current as a function of time - the chronoamperogram - and the spatial distribution of charge as a function of time which can be related to the electrochromic effect in Tezuka's experiments.

For simplicity, in this model, the ionic resistance and the capacitance are assumed constant with oxidation state, which is of course not necessarily the case [8,30]. This assumption seems to be sufficient, however, for qualitative agreement with Tezuka's data, probably because in this geometry, where the electron path-length is thousands of times larger than the ion path-length, the electronic mobility in the reduced state is rate limiting. We find that with reasonable values for the ionic and electronic resistance, the results are relatively independent of the ionic resistance except at short times.

On the other hand, Pickup et. al. [11] used a similar finite difference method to model the case of a thin film of conducting polymer on a conductive substrate. They assume changes to the capacitance and the ionic resistance, but a constant electronic conductivity to get agreement with chronoamperometric data. In theory, all parameters can be measured, and data can be analyzed in any experimental geometry.

3 Results

In this section the model is used to simulate the potentiostatic step experiments performed by Tezuka et. al. The model parameters are found in Table 1. Only the film dimensions and the total film capacitance could be obtained from the experimental data [24]. We used our own measurements of the conductivity of oxidized and reduced films for σ_{max} and σ_{min} . We have no reliable data on the ionic conductivity in polypyrrole, however the conductivity of a good ionic conductor such as polyethylene oxide is approximately $5 \times 10^{-4} \text{S/cm}$ [31] and we estimate that in polypyrrole it will be at least an order of magnitude smaller. The transition potential and width of the conductivity function (Equation 1) as well as the series resistance were obtained from qualitative fits to the data in [22–24].

Figure 3 shows the simulated chronoamperograms for an exhaustively reduced film reoxidized at various potentials. Stepping to potentials greater than the metal-insulator transition potential (0.6V in this model) results in the nearly flat current profile characteristic of a moving phase front, in agreement with

parameter	value
width	$2mm$
length	$6mm$
thickness	$0.91\mu m$
R_S	20Ω
C_V	$2.3mF$
σ_{ion}	$5 \times 10^{-5} \Omega^{-1} cm^{-1}$
σ_{max}	$100 \Omega^{-1} cm^{-1}$
σ_{min}	$0.001 \Omega^{-1} cm^{-1}$
q_0	$0.5 \times q_{max}$
w	$0.05 \times q_{max}$
N	200

Table 1

Test parameters for modeling Tezuka’s experiments. C_V is the total volumetric capacitance, $c = C_V/N$.

data. The slight downward slope of the current in this region is caused by the IR drop down the length of the film. When the front reaches the end of the film, the current decays exponentially. Figure 4 shows the oxidation state of a film as a function of position and time as it is stepped to 1.2V. This figure can be compared to the spectroscopic data presented by Tezuka in [24], and similarly shows a front moving at a constant velocity down the length of the film.

This model shows that the front is simply a shock wave caused by the non-linear transition from the non-conductive to conductive state of the polymer. Charging proceeds as follows: At $t = 0s$, the film is in a highly resistive state, therefore only the capacitor nearest to the working electrode begins to charge. When the charge on this capacitor reaches the transition state, the polymer in this region becomes metallic. This capacitor quickly becomes full and the next capacitor in the series begins to charge. In this way, each capacitor fills sequentially, leading to a constant current with time until the last capacitor reaches the metallic state. The rate of oxidation is determined by the RC time constant, which in this case is dominated by the electronic resistance of the reduced film.

Tezuka et. al. also conclude in their model that electron transfer is the limiting step, but they understand this in terms of the kinetics of charge transfer [25]. The difficulty with this model, however, is that studies of the kinetics of conducting polymers have consistently resulted in unphysical kinetic parameters [32]. In the VRTL model, all the parameters have a straightforward physical

meaning, and should in principle be measurable with a combination of DC electronic conductivity measurements and AC impedance spectroscopy.

Other models predicting fronts in conducting polymer charging have focused on the role of migration on the ion transport through the film [26–29]. Migration in a dielectric medium leads to a constant current and the propagation of a waveform at a constant velocity of $v = \mu E$, where μ is the mobility of the ions, and E is the local electric field at the front boundary. These models conclude that electron transport can not be the limiting mechanism, as electron transport is fast in conducting polymers. This conclusion is based on the fact that these models do not include the capacitive nature of the film. Conducting polymers have an enormous capacitance which will considerably slow the charging, regardless of whether ion or electron motion is limiting. The mass-transport models are also unable to explain why the charging proceeds via fronts during oxidation, but discharges fairly evenly during reduction. In the VRTL model, this phenomenon evolves naturally, with no modification of the parameters or assumptions.

The simulated chronoamperogram for reduction from the fully oxidized state is shown in Figure 5. Because the film is in the highly conductive state to start with, the reduction proceeds evenly over the film and the current decays diffusively like a typical RC transmission line. As in the experimental data, the discharge time is much faster than the charging time because of the initial high conductivity of the film. The small hump observed in the simulated chronoamperogram at very short times is outside of the working range of the model, where effects like the surface capacitance and the charging through the thickness will dominate. The charge evolution during reduction is shown in Figure 6; initially, it decays very quickly but eventually saturates as the film becomes more resistive. The charge gradient along the length of the film at 0.05s is because of the high current at this time, which results in a large IR drop across the film. This was also observed in Tezuka’s experiment [23]. At 7.8s, the current is negligible, however there is a large amount of residual charge in the film not immediately surrounding the working electrode. Tezuka et. al. observe this in [23], and postulate that the discharging stops with a large amount of charge left in the polymer because conductive islands in the polymer are disconnected from one another at a percolation threshold. Figure 6 presents a different explanation. During reduction in this experimental geometry, a small region around the electrode becomes very resistive, preventing further reduction. Contrary to the percolation theory however, in the VRTL model, the rest of the film is more conductive. This could be verified experimentally.

The variable resistance transmission line model also has interesting implications for the interpretation of cyclic voltammograms (CVs) of conducting polymers. In the experimental geometry shown in Figure 1, CVs show an anodic

wave characterized by a sharp peak followed by a constant capacitive current, and a broad cathodic wave. Under increasing scan rate, the anodic peak moves toward higher potential, but the cathodic wave seems relatively unaffected [22]. Normally, peaks in CVs are attributed to a Faradaic reaction. Such peaks are caused by two competing effects: the Maxwell-Boltzmann statistics governing the electron transfer with the electrolyte and diffusion-limited motion of the ions. It is not clear that this picture is applicable to conducting polymers - electron transfer in such a highly interacting system does not proceed via the Nernst equation. This may explain why the observed CVs are difficult to analyze using standard electrochemical theory [30,22,34]. However, in the VRTL model, the shape of conducting polymer CVs is a direct consequence of the metal-insulator transition. The sharp anodic peak is analogous to the front that occurs during oxidation, and the smooth cathodic peak is due to the more diffusive-looking current observed on reduction. The CVs simulated using the parameters from Table 1 are shown in Figure 7 and the results again qualitatively agree with measurement [22]. The model presented here is purely electronic, and presents an alternative explanation for the peaks observed in CVs that seems to be more in keeping with the electronic nature of conducting polymers.

4 Conclusions

Although the metal-insulator transition that occurs during doping of conducting polymers has been known for many years, we present the first electrochemical model to incorporate this phenomenon. The transmission line model, modified to include the oxidation state dependence of the polymer resistance, is able to describe a number of anomalous effects observed in transient experiments, such as moving phase fronts on charging from the fully reduced state, and the persistent charge remaining in the polymer on reduction. The model also reproduces the shape of conducting polymer cyclic voltammograms without relying on the Nernst equation, and is therefore more consistent with the electronic nature of polypyrrole. The transmission line model may be modified to simulate any experimental geometry, provided that the changes in ionic mobility and capacitance with oxidation state can be accurately measured.

References

- [1] K. Frackowiak, K. Jurewicz, S. Delpoux, F. Beguin, F., J. Power Sources 97-98 (2001) 822-825.
- [2] M. Hughes, M.S.P. Shaffer, A.C. Renouf, C. Singh, G.Z. Chen, D.J. Fray, A.

Windle, Adv. Mater. 14 (2002) 382-385.

- [3] S.A. Sapp, G.A. Sotzing, J.R. Reynolds, Chem. Mater. 10 (1998) 2101-2108.
- [4] R.H. Baughman, Science 300 (2003) 268-269.
- [5] R.H. Baughman, Synth. Met. 78 (1996) 339.
- [6] J.D. Madden, N. Wandesteeg, P. Anquetil, P. Madden, A. Takshi, R. Pytel, S. Lafontaine, P. Wieringa, I. Hunter, IEEE J. Ocean. Eng. 29 (2004) 706-728.
- [7] E. Smela, Adv. Mater. 15 (2003) 481-493.
- [8] R.A. Bull, F.F. Fan, A.J. Bard, J. Electrochem. Soc. 129 (1982) 1009-1015.
- [9] R.P. Buck, J. Electroanal. Chem. 210 (1986) 1.
- [10] W.J. Albery, C.M. Elliott, A.R. Mount, J. Electroanal. Chem. 288 (1990) 15.
- [11] P.G. Pickup, Faraday Discuss. Chem. Soc. 88 (1989) 165-176.
- [12] G. Garcia-Belmonte, J. Bisquert, Electrochim. Acta 47 (2002) 4263-4272.
- [13] V. Noël, H. Randriamahazaka, C. Chevrot, J. Electroanal. Chem. 558 (2003) 41-48.
- [14] C. Cachet, R. Wiart, J. Electroanal. Chem. 195 (1985) 21-37.
- [15] B.J. Feldman, P. Burgmayer, R.W. Murray, J. A. Chem. Soc. 107 (1985) 872-878.
- [16] G. Zotti, Synth. Met. 97 (1998) 267-272.
- [17] R. Menon, C.O. Yoon, D. Moses, A.J. Heeger, in: T. Skotheim, R. Elsenbaumer, J. Reynolds (Eds.), Handbook of Conducting Polymers, 2nd Ed., Marcel Dekker, 1998, pp. 27-84.
- [18] M. Winokur, Y.B. Moon, A.J. Heeger, J. Barker, D.C. Bott, H. Shirakawa, Phys. Rev. Lett. 58 (1987) 2329-2332.
- [19] M.R. Warren, J.D. Madden, Organic Thin-Film Electronics, Mater. Res. Soc. Symp. Proc. 871E, I6.1.
- [20] T.F. Otero, H. Grande, J. Rodríguez, J. Electroanal. Chem. 41 (1996) 1863-1869.
- [21] J. Mostany, B.R. Scharifker, Synth. Met. 87 (1997) 179-185.
- [22] Y. Tezuka, K. Aoki, H. Yajima, T. Ishii, J. Electroanal. Chem. 425 (1997) 167-172.
- [23] Y. Tezuka, T. Kimura, T. Ishii, K. Aoki, J. Electroanal. Chem. 395 (1995) 51-55.
- [24] Y. Tezuka, S. Ohyama, T. Ishii, K. Aoki, Chem. Soc. Japan 64 (1991) 2045-2051.
- [25] Y. Tezuka, K. Aoki, K. Shinozaki, Synth. Met. 30 (1989) 369.

- [26] J.C. Lacroix, K. Fraoua, P.C. Lacaze, J. Electroanal. Chem. 444 (1998) 83-93.
- [27] T. Johansson, N. Persson, O. Inganäs, J. Electrochem. Soc. 151 (2004) 119-124.
- [28] X. Wang, B. Shapiro, E. Smela, Adv. Mater. 16 (2004) 1605-1609.
- [29] F. Miomandre, M.N. Bussac, E. Vieil, L. Zuppiroli, Chem. Phys. 255 (2000) 291-300.
- [30] S.W. Feldberg, J. Am. Chem. Soc. 106 (1984) 4671-4674.
- [31] J.Y. Song, Y.Y. Wang, C.C. Wan, J. Power Sources 77 (1999) 183-197.
- [32] K. Aoki, J. Electroanal. Chem. 569 (2004) 121-125.
- [33] E.M. Genies, B. Bidan, A.F. Diaz, J. Electroanal. Chem. 149 (1983) 101.
- [34] P. Marque, J. Roncali, J. Phys. Chem. 94 (1990) 8614-817.

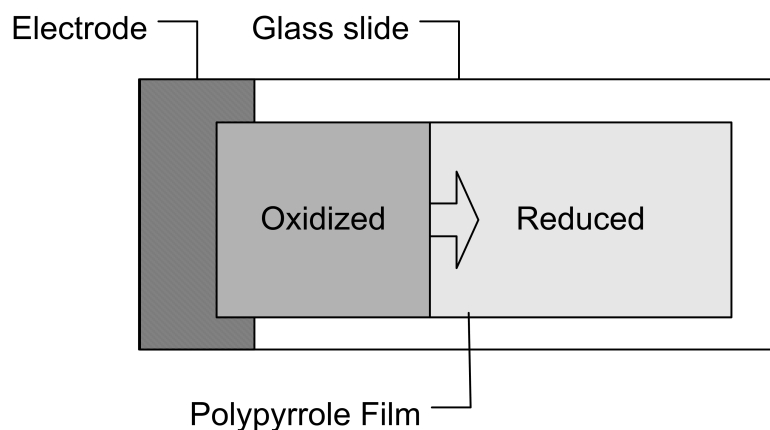


Fig. 1. The working electrode for the experiments of Tezuka et. al. The polypyrrole film is placed on a glass slide, with contact to an ITO working electrode at one end. The figure shows the moving phase front between oxidized and reduced regions that is observed on oxidation from the fully reduced state.

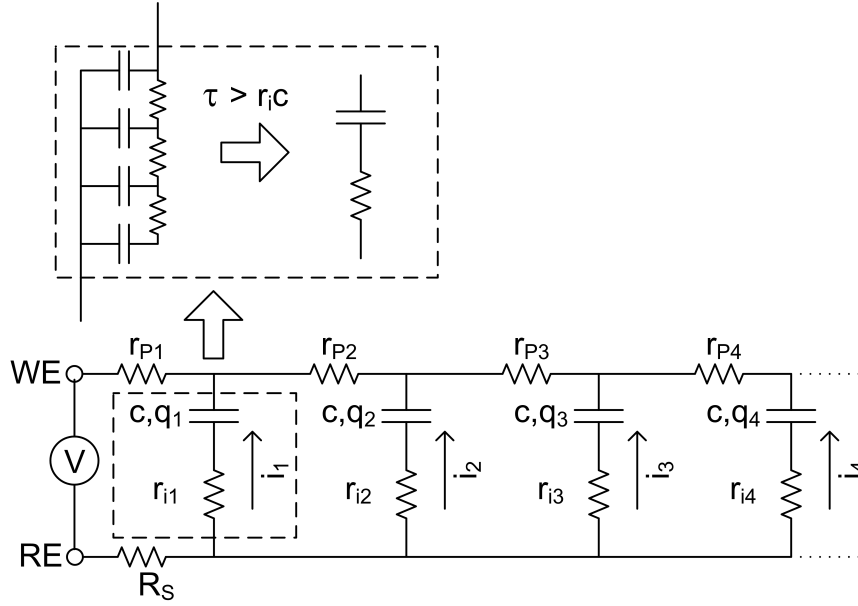


Fig. 2. The transmission line model corresponding to Tezuka's experimental geometry from Figure 1. The top branch is the electron flow, in series through the polymer resistance r_P . The bottom branch is the ion flow, in parallel over the area of the film. The circuit representing charging through the polymer thickness is shown in the dashed box; r_i and c are the ionic resistance and the capacitance per unit length through the thickness, and q is the charge on a capacitor. At time scales longer than $r_i c$, the distributed charging through the thickness can be approximated by a simple RC circuit. R_S is the series resistance in the circuit, including the solution resistance and the contact resistance.

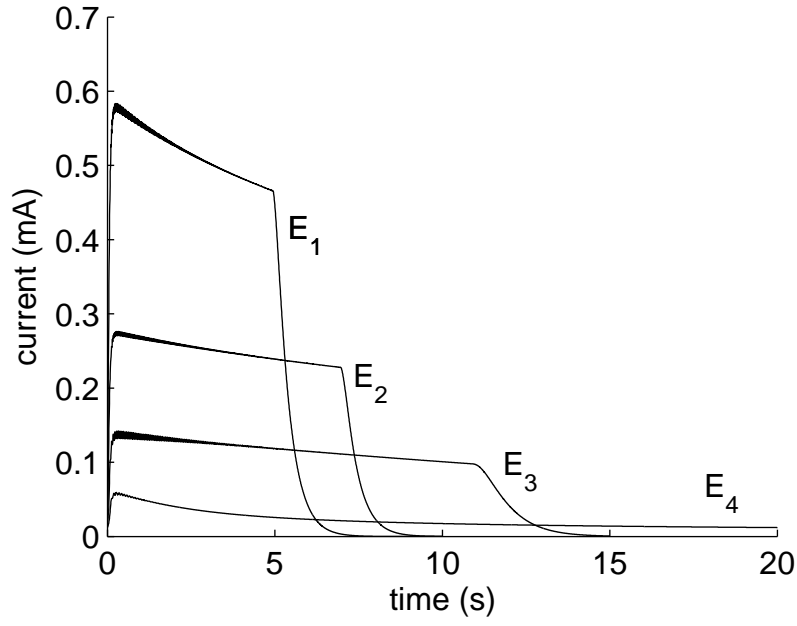


Fig. 3. Chronoamperogram for charging from 0V to 1.2V, 0.8V, 0.6V and 0.4V for E_1 through E_4 respectively. The parameters for the simulation are listed in Table 1. The front current decreases with decreasing overpotential.

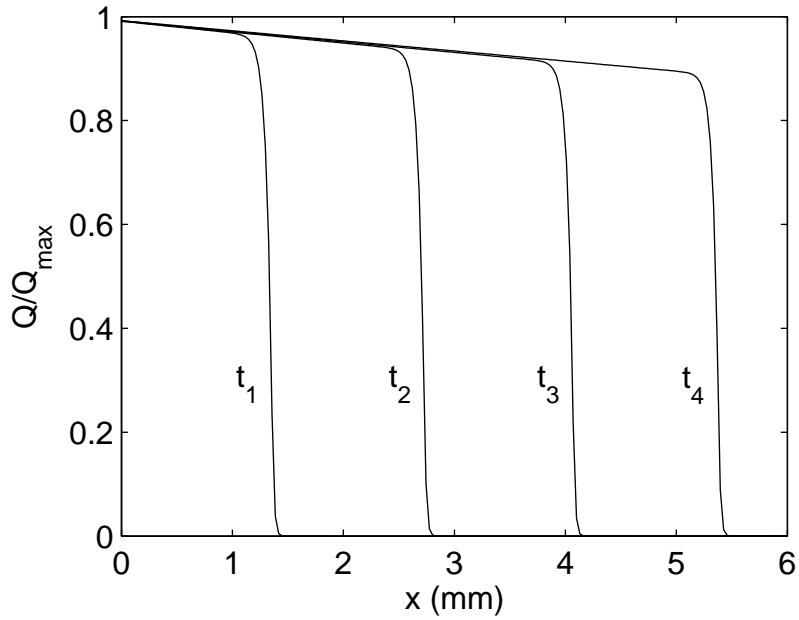


Fig. 4. The spatial distribution of charge during oxidizing from fully reduced clearly shows a front moving at constant velocity along the film. t_1 through t_4 are 1.25s, 2.5s, 3.75s and 5s respectively.

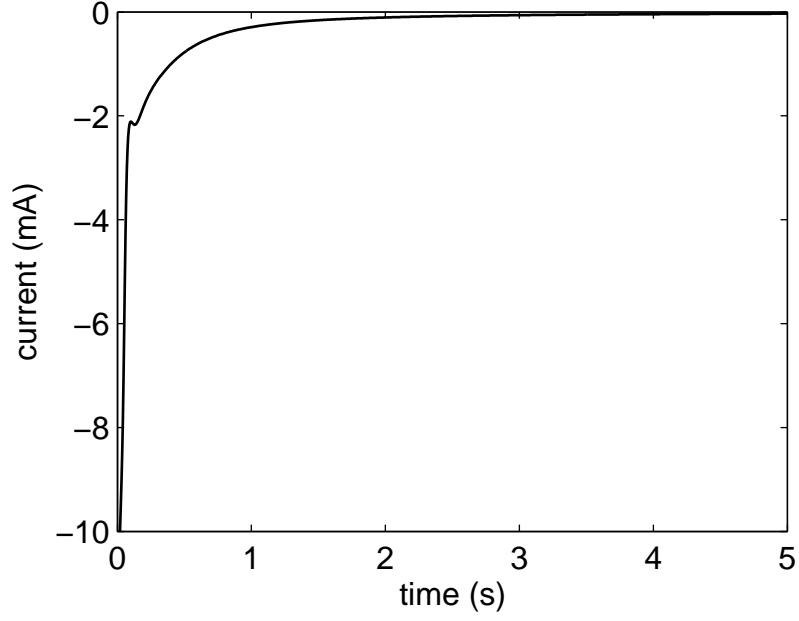


Fig. 5. The modeled chronoamperogram on reducing from fully oxidized.

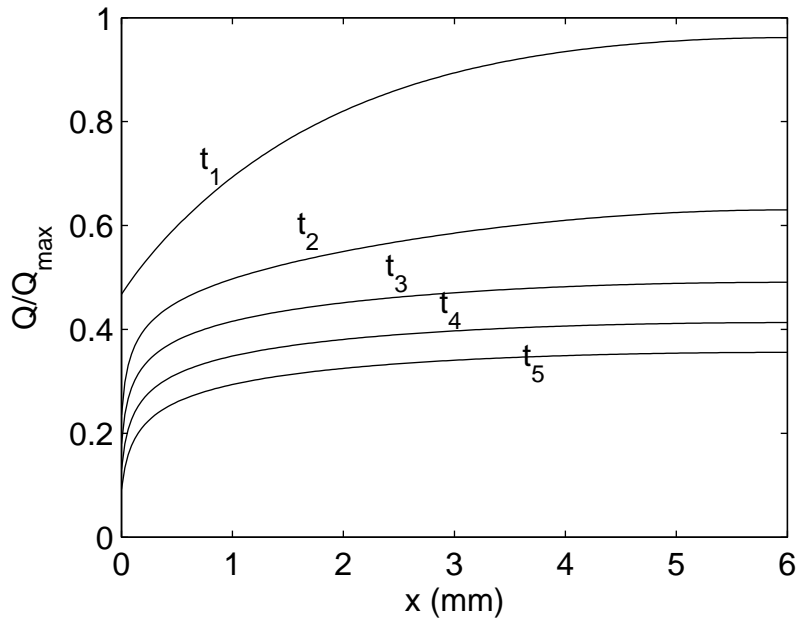


Fig. 6. The spatial distribution of charge during reduction from fully oxidized. t_1 through t_5 are 0.05s, 0.5s, 1.25s, 3.12 and 7.8s respectively. The current is negligible at t_5 , yet approximately 30% of the charge remains through most of the film.

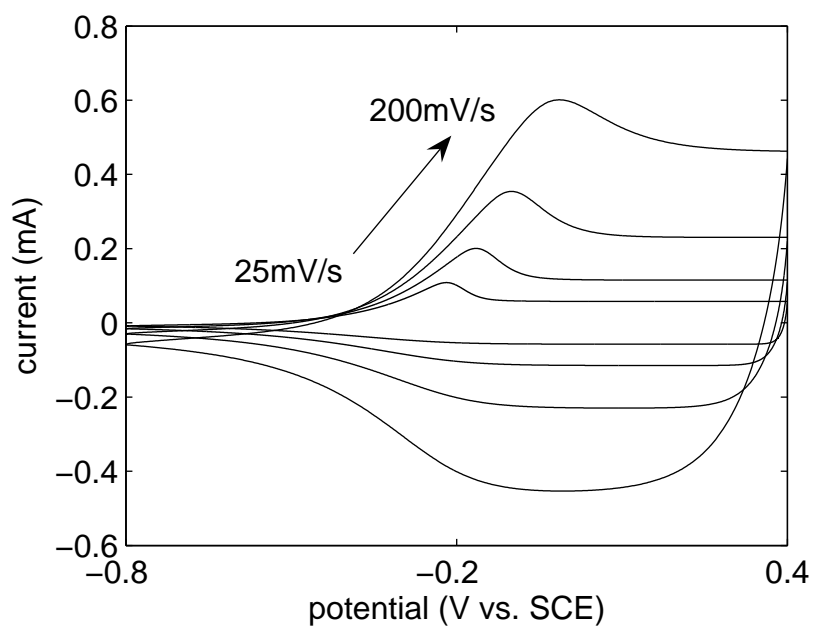


Fig. 7. Simulated cyclic voltammograms of a free-standing film at different rates. The rates are 25mV/s, 50mV/s, 100mV/s and 200mV/s. The clear anodic peak in the simulated CV is due to the metal-insulator transition of the conducting polymer.